Integrated analysis of transcriptome profiling predicts potential lncRNA and circRNA targets in human nasopharyngeal carcinoma

DONG-NI ZHOU[1], CHUN-SHENG YE[2], QING-QING YANG[2] and YAN-FEI DENG[2,3]

Departments of [1]Pathology and [2]Otolaryngology-Head and Neck Surgery, Zhongshan Hospital, Xiamen University, Xiamen, Fujian 361004; [3]Department of Otolaryngology-Head and Neck Surgery, Union School of Clinical Medicine, Fujian Medical University, Fuzhou, Fujian 350001, P.R. China

Received April 10, 2019; Accepted November 8, 2019

DOI: 10.3892/ol.2020.11412

Abstract. Non-coding RNAs (ncRNAs) regulate numerous genes and influence the progression of various human diseases, including cancer. The role of regulatory ncRNAs implicated in nasopharyngeal carcinoma (NPC), as well as their target genes, remains unclear. The present study aimed to investigate specific long non-coding (lnc)RNAs, circular RNAs (circRNAs) and mRNAs associated with the molecular pathogenesis of NPC, and to predict the underlying target genes of specific lncRNAs and circRNAs. The expression levels of lncRNAs, circRNAs and mRNAs in NPC and chronic nasopharyngitis tissues were detected and analyzed using microarray and bioinformatics techniques. A total of 2.80% lncRNAs (425 upregulated and 431 downregulated) were significantly differentially expressed (DE) between the two tissue types. Additionally, 0.96% circRNAs (18 upregulated and 13 downregulated) were significantly DE, while 2.94% mRNAs (426 upregulated and 341 downregulated) were significantly DE between the two tissue types. In total, 420 NPC-associated nearby encoding genes (196 up- and 224 downregulated) of the DE lncRNAs were identified. Overlap analysis identified 23 DE circRNAs and their corresponding target genes, with 37 microRNAs and 50 mRNAs, from which 14 interaction networks were constructed. Subsequent pathway analysis revealed 221 DE target genes corresponding to 31 key signaling pathways associated with NPC, 14 of which may represent hub genes associated with NPC pathophysiology. Thus, certain lncRNAs, circRNAs and mRNAs are aberrantly expressed in NPC tissues, and partially specific lncRNAs, circRNAs and their target genes may influence the tumorigenesis and progression of NPC. Target prediction and regulatory network identification may help to determine the pathogenic mechanisms of NPC.

Correspondence to: Professor Yan-Fei Deng, Department of Otolaryngology-Head and Neck Surgery, Zhongshan Hospital, Xiamen University, 209 Hubin South Road, Xiamen, Fujian 361004, P.R. China
E-mail: dyanfei@139.com

Key words: nasopharyngeal carcinoma, long non-coding RNA, circular RNA, microRNA, mRNA, microarray, bioinformatics analysis

Introduction

Nasopharyngeal carcinoma (NPC) is the most prevalent malignancy in southern China and Southeast Asia. In total, ~129,000 new cases are reported annually worldwide, with >70% reported in South China and Southeast Asia (1). Its pathogenesis is associated with three primary etiological factors; Epstein-Barr virus infection, genetic susceptibility and environmental condition (2). However, the pathophysiological mechanism underlying NPC progression is yet to be elucidated.

Previous studies have predominantly focused on the function of specific genes expressed in NPC instead of the molecular pathogenesis of the disease (1,2). Notably, >98% of human genes are non-protein coding, and the expression of these genes generates non-coding RNAs (ncRNAs) (3). There are multiple families of ncRNA, including ribosomal (r), short interfering (si), micro (mi), circular (circ) and long non-coding (lnc)RNA (4-6). The latter refers to ncRNAs >200 nucleotides in length (4,5). Previous studies have reported that lncRNAs are important regulators of numerous biological processes, including tumor progression (7,8). miRNAs are a class of small ncRNAs of ~22 nucleotides, which serve as key regulators of multiple disease-associated processes (9). Unlike linear RNA, circRNAs exhibit a covalently closed continuous loop, and serve as an miRNA sponge to regulate transcription (10). A number of studies have indicated that ncRNAs play important roles in transcriptional regulation by forming regulatory networks and subsequently interacting with their respective target genes (4-7).

lncRNAs and miRNAs have become increasingly associated with the progression of NPC (11); however, the majority of studies have solely focused on the role of single or small groups of these molecules. Ma *et al* (12) reported that lncRNA HOX transcript antisense RNA contributes towards the tumorigenesis of NPC via the upregulation of fatty acid synthase. Moreover, Zhang *et al* (13) discovered that miRNA-200c acts as an oncogene in NPC, by regulating the phosphatase and tensin homolog genes. To the best of our knowledge, a

limited number of studies to date have investigated the association between circRNA expression and NPC, and no data are currently available concerning circRNAs and their target genes in NPC. Shuai *et al* (14) indicated that circRNA_0000285 may be used as a novel biomarker for NPC radiosensitivity. As the initiation and progression of different types of tumor is a multi-gene, multi-step process, research is typically focused on gene regulatory networks at a genome-wide level.

The purpose of the present study was to comprehensively analyze the expression profiles of lncRNAs, circRNAs and mRNAs in NPC, and their inter-regulatory molecular mechanisms. It was also aimed to identify the target genes of differentially expressed (DE) lncRNAs and circRNAs, and the DE genes (DEGs) within key signaling pathways influencing NPC progression, in order to elucidate the regulatory network in NPC. First, the present study compared the transcriptome profiling of lncRNAs, circRNAs and mRNAs between NPC and chronic nasopharyngitis (CNP) tissues, using microarray technology at the whole genome level. Subsequently, integrated bioinformatics analysis was performed on the three microarray datasets. The results of the present study may help to clarify the associations between lncRNAs, circRNAs and miRNAs (and their target genes), and elucidate the notable regulatory networks involved in the molecular pathogenesis of NPC.

Materials and methods

Specimens. A total of 42 human nasopharyngeal tissue samples were collected from 42 patients (30 men and 12 women) during nasopharyngeal biopsy between August 2013 and October 2014, at Zhongshan Hospital (Ximen, China). The tissue samples included 21 cases of primary NPC and 21 cases of CNP from patients suspected of having cancer. All specimens were confirmed by histopathological examination. Patients did not receive chemoradiotherapy and biotherapy prior to biopsy. The 21 patients with primary NPC comprised 15 men and six women (age range, 20-69 years; median, 45.5 years), and the 21 patients with CNP comprised 16 men and five women (age range, 21-60 years; median, 43.2 years).

All tissues were immediately stored at -80˚C following biopsy, prior to subsequent RNA extraction. Tumor tissues were isolated via micro-dissection and specimens containing >70% tumor cells were further analyzed. In total, six pairs of NPC and CNP specimens among the 42 collected tissues were selected for lncRNA, mRNA and circRNA expression microarray, while all 42 specimens were used for reverse transcription-quantitative (RT-q)PCR. These specimens were used to evaluate differences in the expression levels between NPC and CNP tissues. The present study was approved by the Medical Ethics Committee of Zhongshan Hospital, Xiamen University (Fujian, China) and written informed consent was obtained from all patients prior to the study start.

RNA extraction and quality control. Total RNA was extracted from each tissue sample using TRIzol® reagent (Invitrogen; Thermo Fisher Scientific, Inc.) and purified using the RNeasy Mini kit (Qiagen GmbH), according to the manufacturers' protocol. The quantity and quality of the RNA were determined using a NanoDrop ND-1000 spectrophotometer (NanoDrop Technologies; Thermo Fisher Scientific, Inc.) and the RNA integrity was assessed via electrophoresis on a denaturing agarose gel.

RNA labeling, lncRNA and mRNA microarray. Sample labeling and microarray hybridization were performed using a modified version of the Agilent One-Color Microarray-Based Gene Expression Analysis protocol (Agilent Technologies, Inc.). The rRNA was removed from the total RNA sample using the Ribo-Zero™ rRNA Removal kit (Epicentre; Illumina, Inc.) and mRNA was purified using the mRNA-ONLY™ Eukaryotic mRNA Isolation kit (Epicentre; Illumina, Inc.). Subsequently, each sample was amplified and transcribed into fluorescent cRNA along the entire length of the transcripts, using a random priming method. The labeled cRNAs were purified using the RNeasy Mini kit (Qiagen GmbH), and the concentration and specific activity of the labeled cRNAs [pmol cyanine (Cy)3/μg cRNA] were measured using NanoDrop ND-1000 (NanoDrop Technologies; Thermo Fisher Scientific, Inc.). A total of 0.6 μg of each labeled cRNA was fragmented via the addition of 5 μl 10X blocking agent and 1 μl 25X fragmentation buffer. The mixture was heated at 60˚C for 30 min, and 25 μl 2X GEx hybridization buffer (Agilent Technologies, Inc.) was added to dilute the labeled cRNA. A total of 40 μl hybridization solution was dispensed into a gasket slide and placed into the Human LncRNA Array (version 3.0; 8x60 K; Arraystar, Inc.), which contained 30,586 lncRNAs and 26,109 mRNAs. The slides were incubated for 17 h at 65˚C in an Agilent Microarray hybridization oven. The hybridized arrays were washed with Gene Expression Wash Buffer (Agilent Technologies, Inc.) and subsequently fixed with 3.7% paraformaldehyde for 15 min at room temperature prior to being scanned using the Agilent DNA Microarray Scanner System (G2505C; Agilent Technologies, Inc.).

Agilent Feature Extraction software (version 11.0.1.1; Agilent Technologies, Inc.) was used to analyze the acquired array images. Quantile normalization and subsequent data processing were performed using the GeneSpring GX software package (version 11.5.1; Agilent Technologies, Inc.). Following quantile normalization of the raw data, lncRNAs and mRNAs that were flagged as Present or Marginal ('All Targets Value'), in ≥6 out of 12 samples, were selected for further analyses. Significantly DE lncRNAs and mRNAs (fold-change ≥2.0; P≤0.05) between the two groups were identified via volcano plot filtering. Hierarchical clustering was performed using the Agilent GeneSpring GX software (version 11.5.1; Agilent Technologies, Inc.). Gene Ontology (GO; http://geneontology.org) and Kyoto Encyclopedia of Genes and Genomes (KEGG; http://www.genome.jp/kegg) pathway analyses were performed using the standard enrichment computation method for DE mRNAs. GO analysis was performed in order to characterize genes and gene products in terms of cellular component, molecular function and biological process. KEGG pathway analysis was performed to identify the signaling pathways in which DE mRNAs underwent significant enrichment, and thus predict the underlying biological functions of the DEGs. P<0.05 and the false discovery rate denoted the significance of the GO term enrichment and the biological pathways. The computational data analysis was performed by Kangchen BioTech Co., Ltd.

RNA labeling and circRNA microarray. Sample labeling and Arraystar Human circRNA Array hybridization (Arraystar, Inc.) were performed according to the manufacturer's protocol. Briefly, circRNAs were treated with RNase R (Epicentre; Illumina, Inc.) to remove the linear RNA. Each sample was subsequently amplified and transcribed into fluorescent cRNA using the Arraystar Super RNA Labeling kit (Arraystar, Inc.) and a random priming method. The labeled cRNAs were purified using the RNeasy Mini kit (Qiagen GmbH) and the concentration and specific activity of the labeled cRNAs (pmol Cy3/μg cRNA) was determined using NanoDrop ND-1000 (NanoDrop Technologies; Thermo Fisher Scientific, Inc.). A total of 1 μg of each labeled cRNA was fragmented using 5 μl 10X blocking agent and 1 μl 25X fragmentation buffer. The sample was heated at 60˚C for 30 min, and 25 μl 2X hybridization buffer (Agilent Technologies, Inc.) was added to dilute the labeled cRNAs. A total of 50 μl of hybridization solution was dispensed into a gasket slide and assembled into the Arraystar Human CircRNA Microarray slide (Arraystar, Inc.). The slides were incubated for 17 h at 65˚C in an Agilent hybridization oven. The hybridized arrays were washed with Gene Expression Wash Buffer (Agilent Technologies, Inc.) and subsequently fixed in 3.7% paraformaldehyde for 15 min at room temperature, prior to being scanned using the Agilent Microarray Scanner System (Agilent Technologies, Inc.).

The scanned images were imported into Agilent Feature Extraction software (version 11.0.1.1; Agilent Technologies, Inc.) for raw data extraction. Quantile normalization of the raw data and subsequent data processing were performed using the R software package (version 3.28.0; http://bioconductor.org/packages/edgeR). Low-intensity filtering was performed and circRNAs that were flagged as Present or Marginal ('All Targets Value') in ≥6 out of 12 samples were retained for further analyses. The fold-change between the groups for each circRNA was computed to allow for comparisons between two groups of profile differences (such as cancer vs. inflammation). circRNAs with a fold-change ≥1.5 and P≤0.05 were selected as significantly DE. The analysis outputs were filtered and the DE circRNAs were ranked according to their fold-change and P-value using Microsoft Excel's Data/Sort & Filter functionalities (Microsoft Corporation). The computational data analysis was performed by Kangchen BioTech Co., Ltd.

RT-qPCR validation. Randomly selected DE lncRNAs, mRNAs and circRNAs were evaluated using RT-qPCR. The specific primer sequences for 12 lncRNAs, eight mRNAs and four circRNAs were designed using Primer (version 5.0; Premier Biosoft, Inc.) and are presented in Table SI. The total RNA (1.5 μg) was reverse transcribed into cDNA using the PrimeScript™ RT Reagent kit (Takara Bio, Inc.), according to the manufacturer's protocol. qPCR was performed on a total reaction volume of 10 μl, comprised of 5 μl 2X Master Mix (Arraystar, Inc.), 0.5 μl each of the PCR forward and reverse primers (10 μM), 2 μl DNA and 2 μl double-distilled water. The following thermocycling conditions were used for RT-qPCR: An initial denaturation step of 10 min at 95˚C, followed by 40 cycles of 95˚C for 10 sec and 60˚C for 1 min. All experiments were performed in triplicate. For RT-qPCR validation analysis, all 42 samples were normalized to GAPDH. The fold-change in expression was calculated using the $2^{-\Delta\Delta Cq}$ method (15).

Identification of the nearby coding genes of DE lncRNAs. A nearby coding gene is defined as a coding transcript <300 kb between the DE lncRNA and the neighboring coding mRNA. In the present study, genomic coordinate analysis of DE lncRNAs was performed alongside computational analysis of lncRNA and mRNA microarray data. The NPC-associated DE lncRNAs and their neighboring coding genes were annotated, and genomic coordinates of the lncRNAs, and the association between an lncRNA and its nearby coding gene were also detailed. Additionally, nearby coding genes of DE lncRNAs in NPC were obtained following lncRNA classification, subgroup analysis and genomic coordinate determination.

Predictive analysis of potential targets of DE circRNAs. Overlap analysis was performed via three steps. First, the circRNA-miRNA interaction was predicted with Arraystar's proprietary miRNA target prediction software (version 1.0) using datasets retrieved from the TargetScan and miRanda databases, and the DE circRNAs within all the comparisons were annotated in detail using the circRNA-miRNA interaction information. A total of five target miRNAs for each DE circRNA were subsequently identified according to the number of conservative miRNA binding sites. Subsequently, the candidate target mRNAs for the selected target miRNAs of DE circRNAs were analyzed using Overlap software (version 1.0; Kangchen BioTech Co., Ltd.), based on three miRNA databases (miRanda, miRDB and TargetScan). The intersection of the mRNAs between the aforementioned candidate mRNAs, and the mRNAs in the lncRNA and mRNA microarray data, was determined using Venny software (version 2.1; http://bioinfogp.cnb.csic.es/tools/venny/index.html).

Following the determination of DE circRNAs and their corresponding target genes, the circRNA-miRNA-mRNA regulatory network was constructed and visualized using Cytoscape software (version 3.7.1; http://www.cytoscape.org).

Statistical analysis. The differences in lncRNA, circRNA and mRNA expression levels between NPC and CNP tissues (from the microarray and RT-q-PCR data) were analyzed using the paired Student's t-test, according to their fold-change. Fisher's exact test was used for GO and pathway analyses. P<0.05 was considered to indicate a statistically significant difference. For the microarray analysis, the false discovery rate was calculated to correct the P-value.

Results

Profiles of DE lncRNAs and mRNAs. Among all the lncRNA and mRNA probes in the microarray, 2.80% (856/30,586) lncRNAs (425 upregulated and 431 downregulated) and 2.94% (767/26,109) mRNAs (426 upregulated and 341 downregulated) were significantly DE between the two groups (Tables SII and SIII). The top 20 most significantly DE lncRNAs consisted of more upregulated lncRNAs compared with downregulated lncRNAs (ratio, 16:4). Furthermore, uc004ebm.1 (fold-change, 38.478134) was the most significantly

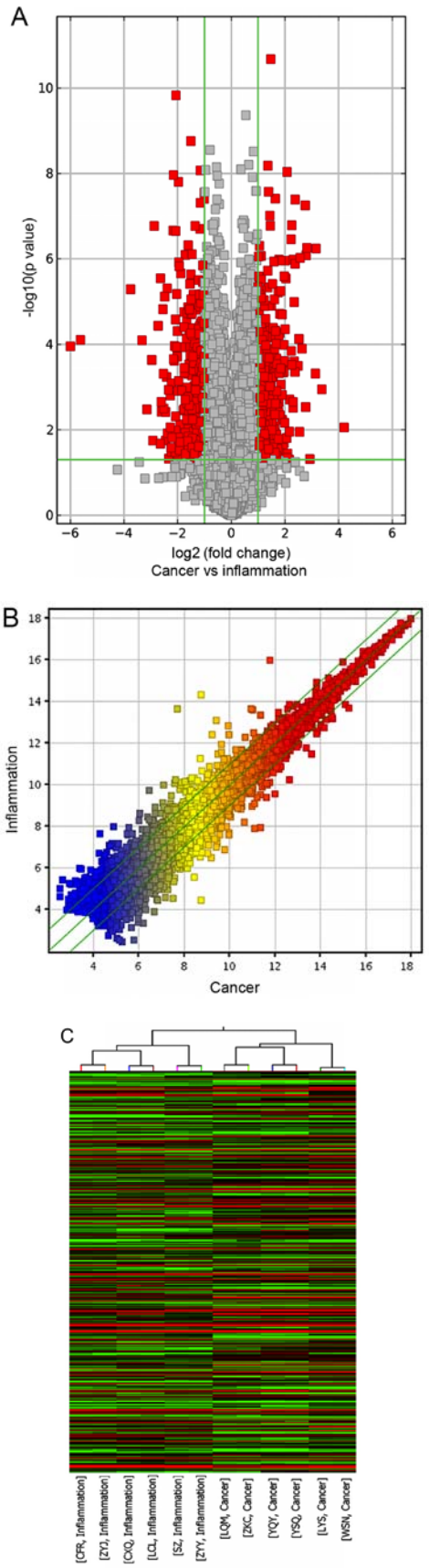

Figure 1. Bioinformatics analysis of differentially expressed mRNAs in NPC and CNP tissues. (A) Volcano plot demonstrating the distribution of mRNAs. (B) Scatter plot exhibiting variation in mRNA expression. (C) Heatmap clustering indicating a distinguishable association between the mRNA expression patterns of certain samples. mRNA expression levels are indicated as follows; Red, high expression and green, low expression. NPC, nasopharyngeal carcinoma; CNP, chronic nasopharyngitis.

upregulated lncRNA, while ENST00000572818 was the most significantly downregulated lncRNA (fold-change, 12.04174). Of the 20 most significantly DE mRNAs; the number of upregulated and downregulated mRNAs were equal (ratio, 10:10). Furthermore, SPRR2E (fold-change, 63.81733) was the most significantly downregulated mRNA, while PCDH10 (fold-change, 18.465176) was the most significantly upregulated mRNA. Differences in mRNA expression between NPC and CNP tissues are presented using a volcano plot, scatter plot and clustering heat-map (Fig. 1A-C, respectively). In addition, pathway analysis revealed that 31 significantly enriched signaling pathways (18 upregulated and 13 downregulated) corresponded to DE mRNAs in this microarray (Tables I, II, SIV and SV).

Profiles of DE circRNAs. In the circRNA microarray, 0.96% of all probes (31 circRNAs, 18 upregulated and 13 downregulated) were significantly DE between the NPC and CNP samples (Tables III and SVI). These comprised two circRNAs (upregulated); hsa_circRNA_100160 (circRNA identifier) and hsa_circRNA_100989, with >6-fold-change differences in expression. The variation of circRNAs between NPC and CNP tissues is presented in a volcano plot, scatter plot and clustering heat map (Fig. 2A-C, respectively).

Validation of selected DE lncRNAs, mRNAs and circRNAs using RT-qPCR. Of the 12 selected DE lncRNAs (NR_027358, ENST00000566575, ENST00000560280, ENST00000411815, ENST00000565929, ENST00000457799, ENST00000514571, ENST00000440518, uc010zye.1, ENST00000443373, ENST00000513638 and ENST00000429469), only ENST00000560280 exhibited significantly opposing microarray expression patterns, which was compared with those resulting from RT-q-PCR analysis. Changes in the expression levels of the other 11 lncRNAs were also verified by RT-q-PCR (Fig. 3A). Of the 8 selected DE mRNAs (SHISA8, XAF1, RORA, MEF2C, TXLNB, MCM2, STAT1 and caspase 3), the expression levels of all except MCM2 exhibited the same trends of up- and downregulation as the microarray data, which indicated a significant difference between NPC and CNP tissues, following RT-qPCR (Fig. 3B). The changes in expression of the four selected DE circRNAs (hsa_circRNA_104204, hsa_circRNA_101252, hsa_circRNA_100160 and hsa_circRNA_001430) were consistent with the results of microarray analysis (Fig. 3C).

Prediction of potential targets of DE lncRNAs. Following bioinformatics and genomic coordinate analyses, the NPC-associated nearby coding genes of DE lncRNAs were listed in the relevant tables (Tables IV, V, SII, SVII and SVIII), including their association and corresponding gene accession number, gene name, protein name, gene strand, gene start location and gene end location. In summary, 420 NPC-associated nearby coding genes, corresponding with DE lncRNAs, were accurately defined and comprised 196 upregulated and 224 downregulated genes.

Prediction of potential targets within significant pathway. In total, 31 significantly enriched signaling pathways (18 associated with upregulated and 13 associated with downregulated

Table I. Key signaling pathways associated with upregulated DEGs.

Pathway ID	Definition	DEGs
hsa04060	Cytokine-cytokine receptor interaction-*Homo sapiens* (human)	CCL2, CCL4, CCR8, CXCL10, CXCL2, CXCL3, CXCL6, CXCR6, EGFR, FAS, GHR, IFNG, IL12A, IL15, IL22RA2, IL23A, LIFR, TNFRSF11B, TNFSF10, TNFSF18
hsa05164	Influenza A-*Homo sapiens* (human)	CCL2, CXCL10, EIF2AK2, FAS, IFIH1, IFNG, IL12A, MX1, OAS1, OAS2, RSAD2, STAT1, TMPRSS13, TNFSF10
hsa05162	Measles-*Homo sapiens* (human)	EIF2AK2, FAS, IFIH1, IFNG, IL12A, MX1, OAS1, OAS2, STAT1, TNFSF10
hsa00260	Glycine, serine and threonine metabolism-*Homo sapiens* (human)	CHDH, GATM, PIPOX, PSAT1, SDS
hsa04630	Jak-STAT signaling pathway-Homo sapiens (human)	GHR, IFNG, IL12A, IL13RA2, IL15, IL22RA2, IL23A, LIFR, SPRY2, STAT1
hsa05160	Hepatitis C-*Homo sapiens* (human)	CLDN1, EGFR, EIF2AK2, IFIT1, OAS1, OAS2, PPP2R2B, PPP2R2C, STAT1
hsa05168	Herpes simplex infection-*Homo sapiens* (human)	CCL2, EIF2AK2, FAS, IFIH1, IFIT1, IFNG, IL12A, IL15, OAS1, OAS2, STAT1
hsa05142	Chagas disease (American trypanosomiasis)-*Homo sapiens* (human)	C1QB, CCL2, FAS, IFNG, IL12A, PPP2R2B, PPP2R2C
hsa04940	Type I diabetes mellitus-*Homo sapiens* (human)	FAS, GAD1, IFNG, IL12A
hsa05144	Malaria-*Homo sapiens* (human)	CCL2, IFNG, IL12A, KLRK1
hsa05412	Arrhythmogenic right ventricular cardiomyopathy (ARVC)-*Homo sapiens* (human)	CACNA2D1, DSG2, DSP, ITGAV, ITGB8
hsa04062	Chemokine signaling pathway-*Homo sapiens* (human)	CCL2, CCL4, CCR8, CXCL10, CXCL2, CXCL3, CXCL6, CXCR6, STAT1
hsa04080	Neuroactive ligand-receptor interaction-*Homo sapiens* (human)	C3AR1, CHRNA7, CHRNB4, EDN1, GABRE, GAL, GHR, GRIN2A, GZMA, LGR5, LHCGR, PPYR1, SSTR2
hsa04066	HIF-1 signaling pathway-*Homo sapiens* (human)	ANGPT2, EDN1, EGFR, IFNG, NOX1, TF
hsa05143	African trypanosomiasis-*Homo sapiens* (human)	FAS, IFNG, IL12A
hsa05410	Hypertrophic cardiomyopathy (HCM)-*Homo sapiens* (human)	CACNA2D1, EDN1, ITGAV, ITGB8, TPM1
hsa04512	ECM-receptor interaction-*Homo sapiens* (human)	COL4A5, ITGAV, ITGB8, LAMA3, LAMB3
hsa05132	Salmonella infection-*Homo sapiens* (human)	CCL4, CXCL2, CXCL3, DYNC1I1, IFNG

DEGs, differentially expressed genes.

genes) were obtained via pathway analysis. Among the 31 signaling pathways corresponding to DE mRNAs, each included a different number of DEGs associated with the pathway identifier. The most significant enrichment pathway was upregulated and included 20 targeted genes associated with 'cytokine-cytokine receptor interaction-*Homo sapiens* (human)'. The least significantly enriched pathways were downregulated and only included two target genes; the target genes, SULT2B1 and SUOX, were involved in 'Sulfur Metabolism-*Homo sapiens* (human)', while the CTSG and MME genes were identified within the 'Renin-angiotensin system-*Homo sapiens* (human)'. In summary, 221 potential target genes are closely associated with 31 key signaling pathways in NPC (Tables I and II).

Prediction of potential target miRNAs of DE circRNAs. All DE circRNAs were annotated in detail with their respective circRNA-miRNA interaction network information (Table SVI). A total of five miRNA response elements for each DE circRNA were predicted from the results of the circRNA microarray (Table III).

Prediction of potential targets of DE circRNAs. In combination with the lncRNA, mRNA and circRNA microarray datasets, the original results of the overlap analysis were exported (Table SIX). Upon induction, 23 DE circRNAs (16 upregulated and 7 downregulated) and their associated target genes (37 miRNAs and 50 mRNAs) were selected. A regulatory network, including 37 circRNA-miRNA interactions and 50 miRNA-mRNA interactions, was then constructed (Table VI and Fig. 4), in which 14 circRNA-miRNA-mRNA regulatory modules were identified (Fig. 5). According to the data, there is no one-to-one correspondence between circRNA and its target genes. For example, hsa_circRNA_104405

Table II. Key signaling pathways associated with downregulated DEGs.

Pathway ID	Definition	DEGs
hsa04640	Hematopoietic cell lineage-*Homo sapiens* (human)	CD19, CD1C, CD22, CD37, CR1, CR2, FCER2, MME, MS4A1
hsa04080	Neuroactive ligand-receptor interaction-*Homo sapiens* (human)	ADRA2A, CNR2, CTSG, EDN3, GALR2, GPR77, GRM5, HTR2A, LEP, MC1R, P2RX5, PRSS1, PRSS3, S1PR4, SCT, TAC4
hsa04662	B cell receptor signaling pathway-*Homo sapiens* (human)	CD19, CD22, CD72, CD79A, CD79B, CR2, VAV3
hsa05217	Basal cell carcinoma - *Homo sapiens* (human)	GLI1, PTCH1, TCF7, WNT16, WNT9A
hsa05340	Primary immunodeficiency-*Homo sapiens* (human)	CD19, CD40LG, CD79A, TNFRSF13C
hsa04340	Hedgehog signaling pathway-*Homo sapiens* (human)	GLI1, PTCH1, WNT16, WNT9A
hsa04064	NF-kappa B signaling pathway-*Homo sapiens* (human)	CCL19, CCL21, CD40LG, CXCL12, TNFRSF13C
hsa00920	Sulfur metabolism-*Homo sapiens* (human)	SULT2B1, SUOX
hsa04614	Renin-angiotensin system-*Homo sapiens* (human)	CTSG, MME
hsa04060	Cytokine-cytokine receptor interaction-*Homo sapiens* (human)	AMHR2, CCL17, CCL19, CCL21, CD40LG, CXCL12, LEP, TNFRSF10D, TNFRSF13C
hsa04062	Chemokine signaling pathway-*Homo sapiens* (human)	CCL17, CCL19, CCL21, CXCL12, GNG7, RASGRP2, VAV3
hsa04672	Intestinal immune network for IgA production-*Homo sapiens* (human)	CD40LG, CXCL12, TNFRSF13C
hsa05030	Cocaine addiction-*Homo sapiens* (human)	CDK5R1, DLG4, FOSB

DEGs, differentially expressed genes.

is associated with 2 target miRNAs (hsa-miR-122-5p and hsa-miR-205-5p), while hsa-miR-122 is associated with 1 target mRNA (RIMS1) and hsa-miR-205-5p is associated with 3 target mRNAs (CENPF, FRK and SCD5).

Discussion

NPC is a type of head and neck cancer with a high incidence and poor overall survival rate, particularly in the endemic regions of Southeast Asia (4). Although a clear understanding of its etiology is yet to be determined, NPC is widely suspected to be the result of both genetic susceptibility, exposure to certain environmental factors or Epstein-Barr virus infection (1,2). Genome-wide association and regulatory ncRNA studies may improve understanding of the etiological and essential molecular mechanisms underpinning NPC progression (14,16,17).

The non-coding regions of the human genome have been closely associated with the biological processes of disease (6). Furthermore, it has been demonstrated that lncRNAs, miRNAs and circRNAs all regulate the physiological and pathological processes of numerous types of cancer, and that these regulatory ncRNAs can affect the functions of their target mRNAs (11,17-19). It has been reported that ncRNA molecules influence tumorigenesis and tumor progression by forming regulatory networks with their target genes (10), which corresponds with the multi-gene and multi-step regulation of tumor development.

Certain studies have investigated the ncRNA regulatory networks that influence the occurrence and development of various types of tumor, including NPC (10,11,13,20). Therefore, in order to delineate an NPC-specific regulatory gene network containing ncRNAs in >10,000 human genes, the comprehensive identification of NPC-associated DE ncRNAs and their targets represents the initial step in establishing this network. To the best of our knowledge, the present study is the first to simultaneously screen and predict the possible target genes of DE ncRNAs (lncRNAs, miRNAs and circRNAs) using three sets of high-throughput microarray data based on transcriptome profiling of NPC tissues. The results constitute a foundation for subsequent comprehensive studies into the regulatory network behind the molecular pathogenesis of NPC.

In the present study, >100 DE lncRNAs and mRNAs were identified in NPC tissues. Subsequently, the NPC-associated nearby coding genes that may represent targets of DE lncRNAs were predicted via bioinformatics analysis, and their associations between DE lncRNAs, nearby coding genes and genome coordinates were also evaluated. Pathway analysis was conducted to determine the biological function of the selected DE mRNAs in NPC pathogenesis, and to predict the essential genes regulating various NPC-associated signaling pathways.

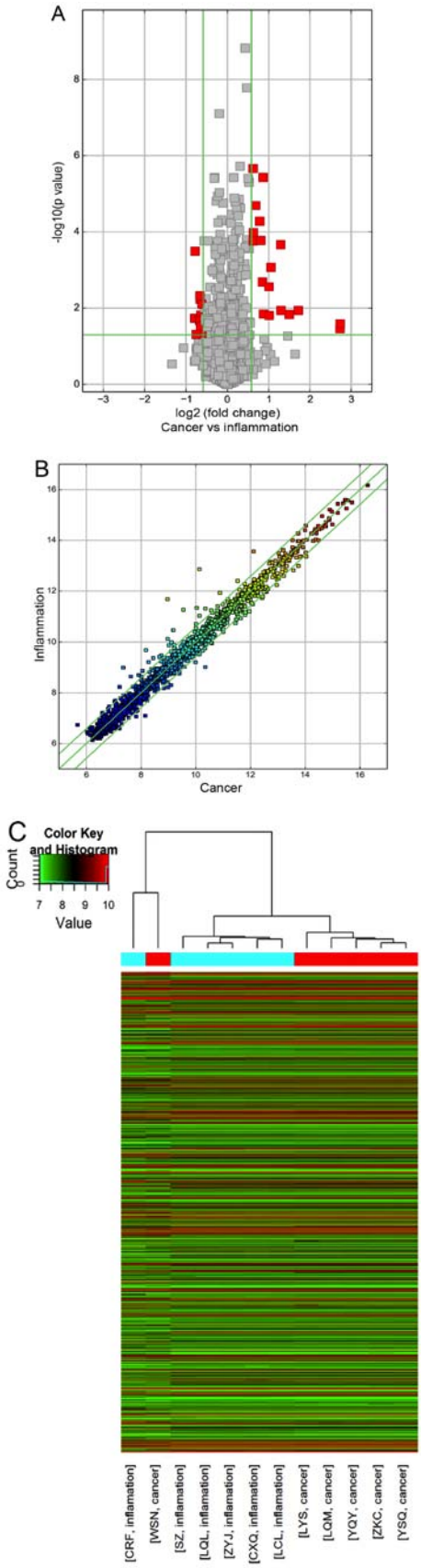

Figure 2. Bioinformatics analysis of differentially expressed circRNAs in NPC and CNP tissues. (A) Volcano plot demonstrating the distribution of circRNAs. (B) Scatter plot exhibiting variation in circRNA expression. (C) Heatmap clustering indicating a distinguishable association between the circRNA expression patterns of certain samples. circRNAs expression levels are indicated as follows; Red, high expression and green, low expression. circRNA, circular RNA; NPC, nasopharyngeal carcinoma; CNP, chronic nasopharyngitis.

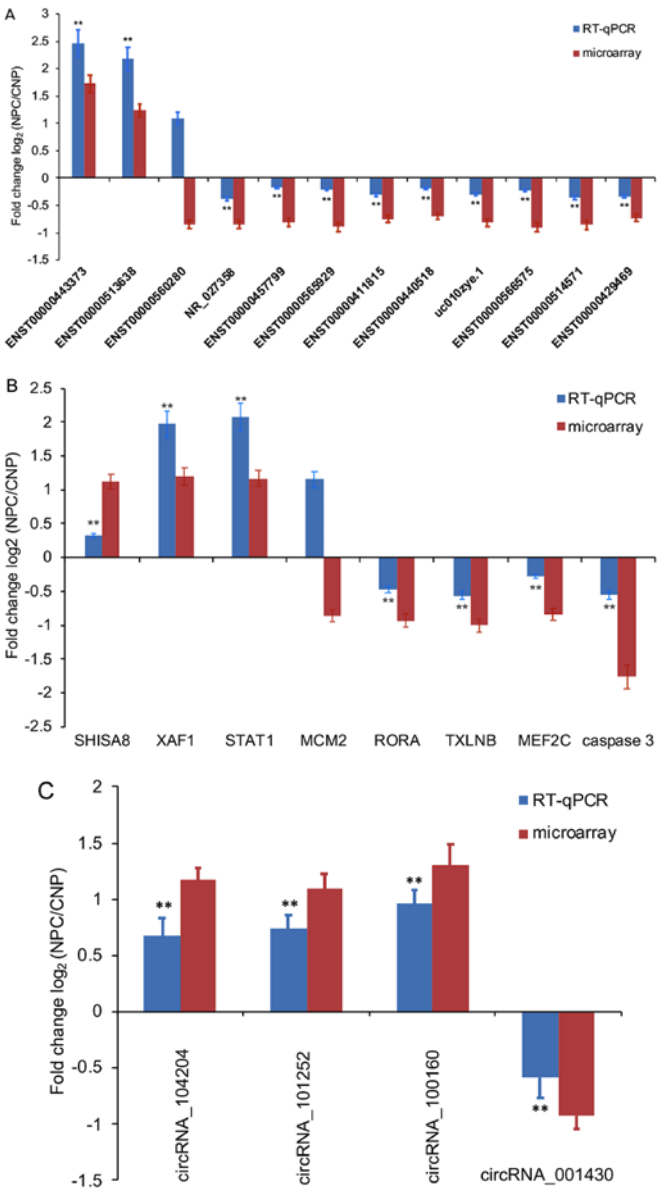

Figure 3. Validation of selected (A) lncRNAs, (B) mRNAs and (C) circRNAs based on microarray and RT-qPCR data. Column heights represent the fold changes (log2 transformed) between NPC and CNP tissues, determined using RT-qPCR and microarray data. The validation results indicated a positive association between the RT-qPCR and microarray data. **P<0.01 vs. microarray. lncRNA, long non-coding RNA; circRNA, circular RNA; RT-qPCR, reverse transcription-quantitative PCR; NPC, nasopharyngeal carcinoma; CNP, chronic nasopharyngitis.

Additional target genes of DE lncRNAs were identified from 31 significantly enriched signaling pathways associated with NPC. The results suggest that aberrantly expressed lncRNAs may influence NPC development and progression through certain mechanisms, such as the interaction between a DE lncRNA and its adjacent protein-coding gene, or via interaction with its target gene in the corresponding signaling pathway. Thus, lncRNA-mRNA networks may serve an important role in the transcriptional regulation of NPC.

Pathway analysis demonstrated that 31 signaling pathways were associated with DEGs, including 18 pathways associated with upregulated, and 13 associated with downregulated genes; three of these pathways ('cytokine-cytokine receptor

Table III. Differentially expressed circRNAs and their miRNA binding sites.

Differentially expressed circRNAs			miRNA binding sites				
circRNA ID	Regulation	Chromosome	MRE1	MRE2	MRE3	MRE4	MRE5
hsa_circRNA_100160	Up	chr 1	hsa-miR-193b-5p	hsa-miR-518a-5p	hsa-miR-527	hsa-miR-1264	hsa-miR-584-3p
hsa_circRNA_100181	Up	chr1	hsa-miR-223-5p	hsa-miR-148a-3p	hsa-miR-148b-3p	hsa-miR-152-3p	hsa-miR-146b-5p
hsa_circRNA_100386	Up	chr1	hsa-miR-193a-5p	hsa-miR-149-3p	hsa-miR-1301-3p	hsa-miR-139-3p	hsa-miR-494-5p
hsa_circRNA_100491	Up	chr1	hsa-miR-223-3p	hsa-miR-26a-5p	hsa-miR-26b-5p	hsa-miR-212-5p	hsa-miR-663a
hsa_circRNA_100989	Up	chr11	hsa-miR-30b-3p	hsa-miR-889-5p	hsa-miR-766-3p	hsa-miR-509-3p	hsa-miR-608
hsa_circRNA_101252	Up	chr13	hsa-miR-762	hsa-miR-654-3p	hsa-miR-1301-3p	hsa-miR-15a-3p	hsa-miR-145-5p
hsa_circRNA_101728	Up	chr16	hsa-miR-518c-5p	hsa-miR-514a-5p	hsa-miR-762	hsa-miR-105-5p	hsa-miR-585-5p
hsa_circRNA_101965	Up	chr17	hsa-miR-519d-5p	hsa-miR-489-3p	hsa-miR-376c-5p	hsa-miR-376b-5p	hsa-miR-298
hsa_circRNA_102539	Up	chr19	hsa-miR-224-3p	hsa-miR-370-3p	hsa-miR-452-5p	hsa-miR-506-3p	hsa-miR-522-3p
hsa_circRNA_102682	Up	chr2	hsa-miR-383-3p	hsa-miR-486-3p	hsa-miR-541-3p	hsa-miR-557	hsa-miR-18a-5p
hsa_circRNA_102817	Up	chr2	hsa-miR-331-5p	hsa-miR-298	hsa-miR-296-3p	hsa-miR-30c-1-3p	hsa-miR-588
hsa_circRNA_103578	Up	chr4	hsa-miR-149-5p	hsa-miR-650	hsa-miR-548a-3p	hsa-miR-148b-5p	hsa-miR-589-3p
hsa_circRNA_103964	Up	chr5	hsa-miR-512-3p	hsa-miR-215-3p	hsa-miR-492	hsa-miR-105-5p	hsa-miR-200a-3p
hsa_circRNA_103965	Up	chr5	hsa-miR-512-3p	hsa-miR-215-3p	hsa-miR-492	hsa-miR-105-5p	hsa-miR-377-3p
hsa_circRNA_104204	Up	chr6	hsa-miR-619-5p	hsa-miR-370-3p	hsa-miR-448	hsa-miR-18b-5p	hsa-miR-18a-5p
hsa_circRNA_104244	Up	chr6	hsa-miR-892b	hsa-miR-149-5p	hsa-miR-130b-5p	hsa-miR-1271-3p	hsa-miR-432-3p
hsa_circRNA_104405	Up	chr7	hsa-miR-122-5p	hsa-miR-205-5p	hsa-miR-136-5p	hsa-miR-214-3p	hsa-miR-138-5p
hsa_circRNA_104589	Up	chr8	hsa-miR-511-5p	hsa-miR-548d-5p	hsa-miR-548b-5p	hsa-miR-548c-5p	hsa-miR-658
hsa_circRNA_000250	Down	chr18	hsa-miR-181c-5p	hsa-miR-181b-5p	hsa-miR-181d-5p	hsa-miR-224-3p	hsa-miR-181a-5p
hsa_circRNA_000526	Down	chr10	hsa-miR-92a-2-5p	hsa-miR-488-5p	hsa-miR-542-3p	hsa-miR-525-5p	hsa-miR-193b-5p
hsa_circRNA_001430	Down	chr5	hsa-miR-92a-2-5p	hsa-miR-491-5p	hsa-miR-16-5p	hsa-let-7g-5p	hsa-miR-193a-5p
hsa_circRNA_100044	Down	chr1	hsa-miR-629-3p	hsa-miR-486-3p	hsa-miR-134-3p	hsa-miR-877-3p	hsa-miR-377-5p
hsa_circRNA_100499	Down	chr1	hsa-miR-504-3p	hsa-miR-21-5p	hsa-miR-337-3p	hsa-miR-642a-5p	hsa-miR-16-2-3p
hsa_circRNA_101969	Down	chr17	hsa-miR-18a-3p	hsa-miR-519a-5p	hsa-miR-519b-5p	hsa-miR-519c-5p	hsa-miR-518e-5p
hsa_circRNA_102062	Down	chr17	hsa-miR-18a-5p	hsa-miR-485-5p	hsa-miR-150-3p	hsa-miR-433-5p	hsa-miR-18b-5p
hsa_circRNA_102113	Down	chr17	hsa-miR-106b-3p	hsa-miR-545-5p	hsa-miR-766-5p	hsa-miR-660-3p	hsa-miR-625-5p
hsa_circRNA_102224	Down	chr17	hsa-miR-17-3p	hsa-miR-520g-3p	hsa-miR-422a	hsa-miR-520h	hsa-miR-545-3p
hsa_circRNA_102226	Down	chr17	hsa-miR-17-3p	hsa-miR-802	hsa-miR-495-3p	hsa-miR-143-5p	hsa-miR-516b-5p
hsa_circRNA_102535	Down	chr19	hsa-miR-221-5p	hsa-miR-431-5p	hsa-miR-602	hsa-miR-662	hsa-miR-661
hsa_circRNA_103992	Down	chr5	hsa-miR-1301-3p	hsa-miR-130b-5p	hsa-miR-204-3p	hsa-miR-29b-1-5p	hsa-miR-877-3p
hsa_circRNA_104652	Down	chr8	hsa-miR-25-3p	hsa-miR-512-3p	hsa-miR-134-5p	hsa-miR-134-3p	hsa-let-7i-5p

circRNA, circular RNA; miRNA, micro RNA; MRE, miRNA recognition elements.

Table IV. Nearby coding genes for long intergenic non-coding RNAs.

Sequence name	Gene symbol	Genomic location	GR	Nearby gene
AW833912		Chr 3: 172556888-172557496	D	NM_018098
BF108976		Chr 2: 192068946-192069452	D	NM_007315
BG953017R		Chr 4: 184736396-184736595	U	ENST00000296741
ENST00000400353	AP000569.8	Chr 21: 35303517-35343487	U	NM_001001132
ENST00000411844	KIAA0664L3	Chr 16: 3171560031717339	U	ENST00000389202
ENST00000412797	RP11-70P17.1	Chr 1: 25907968-25916847	D	NM_024037
ENST00000413991	AC073257.2	Chr 2: 121300484-121301902	U	NM_005270
ENST00000420672	AC009948.5	Chr 2: 179278665-179295551	U	NM_145739
ENST00000425214	CCDC144B	Chr 17: 18494172-18507053	U	NM_016078
ENST00000431729	RP11-191N8.2	Chr 1: 222001007-222014008	D	NM_144729
ENST00000434893	GUSBP11	Chr 22: 23995356-24029101	U	NM_013378
ENST00000438082	RP11-57C13.6	Chr 10: 89367741-89419036	D	NM_004670
ENST00000439051	RP11-57C13.6	Chr 10: 89367768-89419036	D	NM_004670
ENST00000439472	TTTY10	Chr Y: 22669139-22680293	U	NM_001039567
ENST00000440357	RP4-738P15.1	Chr 20: 25124000-25129876	D	ENST00000480798
ENST00000441287	AC011193.1	Chr 17: 32806352-32806976	U	NM_002982
ENST00000442583	CCDC144B	Chr 17: 18491592-18509704	U	NM_016078
ENST00000449023	SRGAP3-AS4	Chr 3: 9298442-9299191	U	NM_014850
ENST00000457217	RP11-222A5.1	Chr 1: 175846478-175849604	U	NM_003285
ENST00000483245	RP11-202A13.1	Chr 3: 133774099-133776492	D	NM_001063
ENST00000486295	EGFEM1P	Chr 3: 168538977-168547319	D	ENST00000264674
ENST00000514571	CTC-454M9.1	Chr 5: 88261691-88464485	U	NM_001193347
ENST00000520323	CTB-11I22.2	Chr 5: 158654722-158672135	U	NM_024007
ENST00000520840	RP11-875O11.3	Chr 8: 22928889-22932001	U	ENST00000312584
ENST00000536112	RP11-81H14.2	Chr 12: 68825634-68826434	D	NM_000619
ENST00000537192	RP11-1038A11.3	Chr 12: 5399645-5487520	D	NM_002527
ENST00000538430	RP11-1038A11.1	Chr 12: 5497754-5515817	D	NM_002527
ENST00000539404	RP11-81H14.2	Chr 12: 68726727-68797580	D	NM_000619
ENST00000541707	RP11-81H14.2	Chr 12: 68726667-68729561	D	NM_000619
ENST00000544591	RP11-291B21.2	Chr 12: 10705961-10710648	U	NM_007333
ENST00000544842	RP11-319E16.2	Chr 12: 5425126-5428513	D	NM_002527
ENST00000546086	RP11-81H14.2	Chr 12: 68727032-68835996	D	NM_000619
ENST00000546968	RP11-44N21.1	Chr 14: 105561527-105565341	U	NM_138790
ENST00000548846	RP3-473L9.4	Chr 12: 111834638-111841111	D	NM_001136538
ENST00000549710	RP11-498M15.1	Chr 12: 72102950-72104154	D	NM_003667
ENST00000552154	RP11-554D14.7	Chr 12: 108226634-108228807	D	ENST00000342331
ENST00000556624	RP11-219E7.1	Chr 14: 21252046-21252452	D	ENST00000298687
ENST00000558147	LINC00277	Chr 15; 69373189-69383734	U	ENST00000310673
ENST00000558419	CTD-2008A1.1	Chr 15: 45118737-45119292	D	NM_003104
ENST00000559914	LINC00277	Chr 15: 69365277-69367206	U	ENST00000310673
ENST00000561384	CTD-2008A1.2	Chr 15: 45119397-45176892	U	NM_003104
ENST00000562834	RP3-523K23.2	Chr 6: 54807964-54809897	U	NM_001010872
ENST00000563852	RP11-506G7.1	Chr 17: 41020507-41025481	D	NM_007299
ENST00000564832	RP11-531A24.3	Chr 8: 73859384-73862680	D	NM_001243237
ENST00000566575	CTA-250D10.23	Chr 22: 42318026-42319104	D	NM_001207020
ENST00000568337	RP11-160C18.2	Chr 15: 79021382-79026298	U	NM_000750
ENST00000569215	RP11-609N14.1	Chr 16: 10445296-10446609	D	NM_001134407
ENST00000569655	RP11-143K11.1	Chr 17: 71171621-71172772	U	NM_001050
ENST00000569892	RP11-114H24.3	Chr 15: 78246416-78255996	U	NM_015162
ENST00000575693	LA16c-325D7.2	Chr 16: 2916348-2917619	U	NM_024507
ENST00000577807	RP11-599B13.3	Chr 17: 7959542-7960939	D	NM_001039131
HMlincRNA791-	HMlincRNA791	Chr 18: 52298998-52308760	U	NM_001143829

Table IV. Continued.

Sequence name	Gene symbol	Genomic location	GR	Nearby gene
HMlincRNA963+	HMlincRNA963	Chr 3: 168554930-168560248	D	ENST00000264674
NR_024475	LOC100216001	Chr 10: 4692376-4720262	U	NM_001353
NR_026878	FOXD2-AS1	Chr 1: 47897806-47900313	D	ENST00000337817
NR_027994	NHEG1	Chr 6: 137303295-137314368	U	NM_181310
NR_038293	LOC100507173	Chr 6: 27661813-27678001	D	ENST00000331442
NR_040109	LOC100505495	Chr 19: 41960073-42006554	U	NM_006890
TCONS_00001315	XLOC_000595	Chr 1: 227976987-227979782	D	NM_003395
TCONS_00001451	XLOC_000781	Chr 1: 35081179-35083207	U	NM_005268
TCONS_00005258	XLOC_002368	Chr 2: 160780449-160792478	U	NM_001007267
TCONS_00005268	XLOC_002383	Chr 2: 169197716-169198115	U	NM_203463
TCONS_00006514	XLOC_003131	Chr 3: 54048256-54065456	D	NM_018397
TCONS_00008529	XLOC_004016	Chr 4: 90459366-90472707	U	ENST00000420646
TCONS_00009933	XLOC_004361	Chr 5: 42922835-42924839	U	NM_000163
TCONS_00010742	XLOC_004475	Chr 5: 92906525-92909378	D	NM_005654
TCONS_00011633	XLOC_005123	Chr 6: 1489677-1490173	U	NM_033260
TCONS_00011758	XLOC_005220	Chr 6: 27677988-27680876	D	ENST00000331442
TCONS_00012442	XLOC_005214	Chr 6: 26674955-26677930	U	NM_001732
TCONS_00012443	XLOC_005214	Chr 6: 26675224-26688063	U	NM_001732
TCONS_00014617	XLOC_006712	Chr 8: 11500332-11506826	U	NM_001715
TCONS_00014681	XLOC_006779	Chr 8: 39891375-39891902	U	NM_001464
TCONS_00017282	XLOC_008100	Chr X: 2484083-2488088	U	NM_001141919
TCONS_00017293	XLOC_008116	Chr X: 13405670-13437996	U	NM_001167890
TCONS_00018417	XLOC_008704	Chr 10: 4790106-4806336	U	NM_001353
TCONS_00021032	XLOC_009637	Chr 12: 7491433-7494514	U	NM_031491
TCONS_00021064	XLOC_009662	Chr 12: 10725616-10727581	U	NM_007333
TCONS_00029036	XLOC_013955	Chr 21: 44232379-44237997	U	NM_001001568
TCONS_00029753	XLOC_014147	Chr 22: 18848963-18851914	U	NM_017414
TCONS_00029855	XLOC_014297	Chr 22: 19543858-19552723	D	NM_001178010
uc001yfd.1	BX247990	Chr 14: 96181819-96223116	D	NM_001252507
uc002ebp.1	TRIM72	Chr 16: 31237192-31237830	D	ENST00000389202
uc002iby.2	LOC388387	Chr 17: 41026690-41050751	D	NM_001158
uc002nbr.3	UCA1	Chr 19: 15939756-15946230	D	ENST00000344824
uc002zbk.2	BC041455	Chr 21: 44019513-44035168	U	NM_001001568
.uc002zob.1	GGT3P	Chr 22: 18761201-18792992	D	NM_017414
uc003fif.1	AK127557	Chr 3: 172308502-172312373	D	ENST00000241261
uc003ihb.3	BC042378	Chr 4: 134114523-134115760	U	ENST00000264360
uc003qhh.4	NHEG1	Chr 6: 137303295-137314368	U	NM_181310
uc010jbc.2	FLJ42709	Chr 5: 92877577-92916738	U	NM_005654
uc010vdm.1	RRN3P2	Chr 16: 29086162-29107582	U	NM_001178098

Chr, chromosome; GR, genome relationship; U, upstream; D, downstream.

interaction', 'chemokine signaling pathway' and 'neuroactive ligand-receptor interaction') were simultaneously associated with upregulated and downregulated signaling pathways. Of the 74 target genes associated with the above three pathways, 14 genes (LEP, CCL17, CCL19, CCL21, CXCL12, CCL2, CCL4, CCR8, CXCL10, CXCL2, CXCL3, CXCL6, CXCR6 and GHR) were separately involved in ≥2 of these pathways. The functions of these target genes were associated with the following biological processes: 'Signal transduction', 'cell adhesion and migration', 'cell proliferation', 'inflammatory cell infiltration', 'angiogenesis' and 'immunoregulation'. Additionally, various pathways and target genes were associated with the development and progression of several other human cancer types (21-23). The present results indicate that the three aforementioned pathways, and 14 identified genes, may represent key regulators of NPC tumorigenesis.

Additionally, multiple DE circRNAs associated with NPC, and their target miRNAs/mRNAs, were investigated

Table V. Nearby coding genes for enhancer long non-coding RNAs.

Sequence name	Gene symbol	Genomic location	GR	Nearby gene
ENST00000400353	AP000569.8	Chr 21: 35303517-35343487	U	NM_001001132
ENST00000411844	KIAA0664L3	Chr 16: 31715600-31717339	U	ENST00000389202
ENST00000412797	RP11-70P17.1	Chr 1: 25907968-25916847	D	NM_024037
ENST00000431729	RP11-191N8.2	Chr 1: 222001007-222014008	D	NM_144729
ENST00000440357	RP4-738P15.1	Chr 20: 25124000-25129876	D	ENST00000480798
ENST00000440357	RP4-738P15.1	Chr 20: 25124000-25129876	U	NM_021067
ENST00000441287	AC011193.1	Chr 17: 32806352-32806976	U	NM_002982
NR_024475	LOC100216001	Chr 10: 4692376-4720262	U	NM_001353
NR_026878	FOXD2-AS1	Chr 1: 47897806-47900313	D	ENST00000337817
NR_027994	NHEG1	Chr 6: 137303295-137314368	U	NM_181310
uc003qhh.4	NHEG1	Chr 6: 137303295-137314368	U	NM_181310

Chr, chromosome; GR, genome relationship; U, upstream; D, downstream.

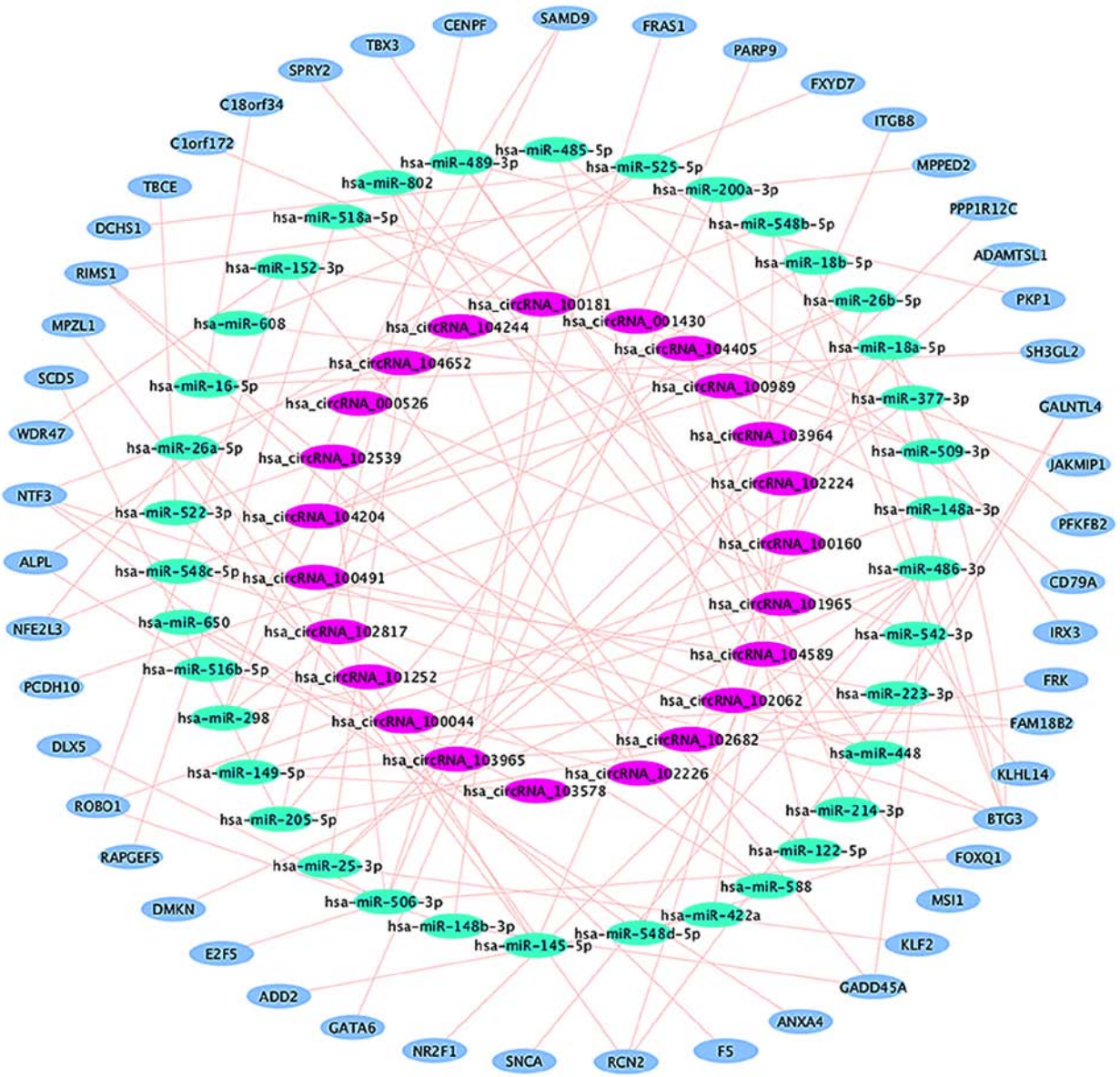

Figure 4. circRNA-miRNA-mRNA regulatory network in nasopharyngeal carcinoma. Green circle, miRNA; pink circle, circRNA; light-blue circle, mRNA. circRNA, circular RNA; miRNA, micro RNA.

Table VI. Regulatory network components of differentially expressed circRNAs in nasopharyngeal carcinoma.

circRNA identifier	Regulation	miRNA	mRNA
hsa_circRNA_100181	Up	hsa-miR-148a-3p	GADD45A, ROBO1
		hsa-miR-148b-3p	GADD45A, ROBO1
		hsa-miR-152-3p	GADD45A, ROBO1, WDR47
hsa_circRNA_104405	Up	hsa-miR-122-5p	RIMS1
		hsa-miR-205-5p	CENPF, FRK, SCD5
		hsa-miR-214-3p	GALNTL4
hsa_circRNA_102682	Up	hsa-miR-486-3p	SNCA
		hsa-miR-18a-5p	BTG3
hsa_circRNA_102539	Up	hsa-miR-506-3p	DLX5, E2F5, FOXQ1, FRAS1, PARP9
		hsa-miR-522-3p	F5, TBCE
hsa_circRNA_103578	Up	hsa-miR-149-5p	FAM18B2
		hsa-miR-650	ANXA4
hsa_circRNA_101252	Up	hsa-miR-145-5p	ITGB8, MPZL1
hsa_circRNA_101965	Up	hsa-miR-489-3p	PKP1
		hsa-miR-298	SAMD9
hsa_circRNA_103965	Up	hsa-miR-377-3p	IRX3, PCDH10
hsa_circRNA_104204	Up	hsa-miR-448	BTG3, NTF3, SPRY2, TBX3
		hsa-miR-18b-5p	BTG3
		hsa-miR-18a-5p	BTG3
hsa_circRNA_102817	Up	hsa-miR-298	SAMD9
		hsa-miR-588	RIMS1
hsa_circRNA_104244	Up	hsa-miR-149-5p	FAM18B2
hsa_circRNA_103964	Up	hsa-miR-200a-3p	GATA6, MPPED2, RIMS1
hsa_circRNA_100989	Up	hsa-miR-509-3p	C1orf172
		hsa-miR-608	FXYD7
hsa_circRNA_100160	Up	hsa-miR-518a-5p	JAKMIP1, RAPGEF5
hsa_circRNA_100491	Up	hsa-miR-223-3p	GALNTL4, RCN2
		hsa-miR-26a-5p	NFE2L3, RCN2
		hsa-miR-26b-5p	NFE2L3, RCN2
hsa_circRNA_104589	Up	hsa-miR-548d-5p	BTG3, NTF3
		hsa-miR-548b-5p	BTG3, NTF3
		hsa-miR-548c-5p	BTG3, NTF3
hsa_circRNA_100044	Down	hsa-miR-486-3p	DMKN, NR2F1
hsa_circRNA_104652	Down	hsa-miR-25-3p	ADAMTSL1, KLF2, PPP1R12C
hsa_circRNA_000526	Down	hsa-miR-542-3p	KLHL14
		hsa-miR-525-5p	ALPL, DCHS1, PFKFB2
hsa_circRNA_001430	Down	hsa-miR-16-5p	C18orf34, SH3GL2
hsa_circRNA_102062	Down	hsa-miR-485-5p	CD79A
hsa_circRNA_102224	Down	hsa-miR-422a	ADD2
hsa_circRNA_102226	Down	hsa-miR-802	MSI1
		hsa-miR-516b-5p	ALPL

circRNA, circular RNA; miRNA/miR, micro RNA.

alongside their corresponding association and genome mapping. However, thus far, no detailed reports are available on the association between circRNAs and their targets in NPC. The present study identified regulatory circRNA-miRNA-mRNA networks in NPC, which contained different modules consisting of relevant target genes. The current results indicate that aberrantly expressed circRNAs may influence different pathophysiological mechanisms of NPC via interaction with miRNAs and mRNAs, and also that the circRNA-miRNA-mRNA motifs serve a key regulatory

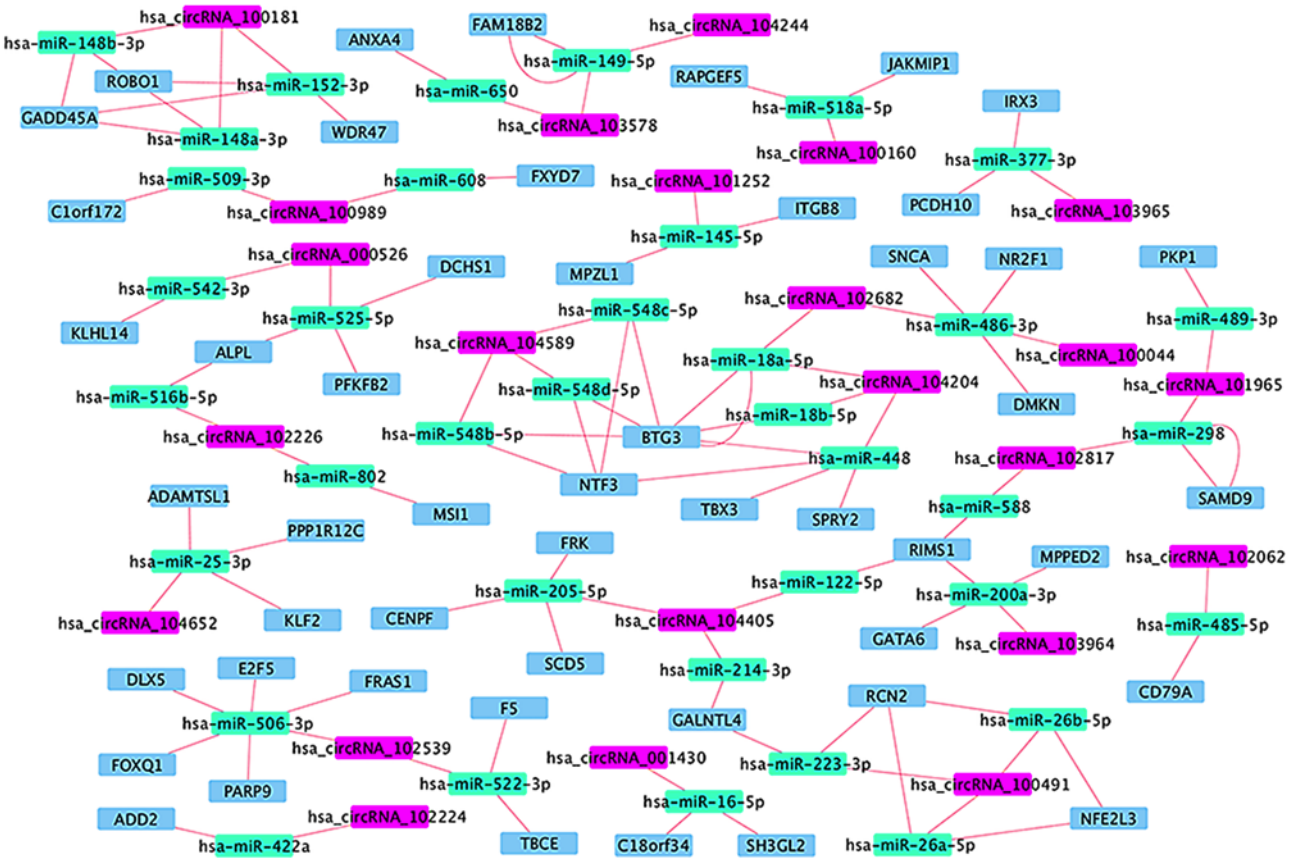

Figure 5. circRNA-miRNA-mRNA regulatory modules in nasopharyngeal carcinoma. Green rectangle, miRNA; pink rectangle, circRNA; light-blue rectangle, mRNA. circRNA, circular RNA; miRNA, micro RNA.

function in NPC. Taken together, the present data indicate that lncRNAs do not serve an isolated role, but target the mRNAs of various other genes, and influence other associated genes involved in the tumorigenesis and progression of NPC, by forming regulatory networks.

In the circRNA-miRNA-mRNA network, 50 mRNAs were identified as the final functional genes. According to the National Center for Biotechnology Information gene database, the functions of these target genes were associated with the following physiological and pathological mechanisms: 'Environmental stress', 'cell motility and migration', 'cytoskeleton', 'antiproliferative activity', 'regulation of voltage-gated calcium channels', 'cell proliferation and apoptosis', 'desmosome formation', 'annexin', 'B lymphocyte antigen receptor' 'bimodal regulator of epidermal growth factor receptor and mitogen-activated protein kinase signaling', 'extracellular matrix protein' and 'chromosome segregation'. Notably, previous studies have revealed that certain identified target genes are associated with cancer cell proliferation and metastasis (24,25), and thus serve important roles in NPC development and progression (26-28).

Overall, the present study simultaneously identified DE lncRNAs, circRNAs and mRNAs between NPC and CNP tissues via the integrated analysis of three transcriptome profiling datasets. Furthermore, potential target genes for these DE ncRNAs, and key signaling pathways associated with NPC, were identified using bioinformatics analysis. Finally, possible regulatory networks comprised of different modules in NPC were predicted and constructed. The present study serves to evaluate the association between these genes and NPC at the RNA transcriptome level. It also provides novel information to elucidate the molecular pathogenesis of NPC from a networking perspective. In further studies, the biological functions of these regulatory networks in NPC should be verified.

Acknowledgements

Not applicable.

Funding

The present study was funded by the Natural Science Fund of Fujian Province, China (grant no. 2017J01374).

Availability of data and materials

All data generated or analyzed during this study are included in this published article.

Authors' contributions

YFD designed the study. YFD and CSY revised the manuscript. DNZ, CSY and QQY performed the research, collected and analyzed the data, and wrote the manuscript. All authors read and approved the final manuscript.

Ethics approval and consent to participate

The present study was ethically approved by the Medical Ethics Committee of Zhongshan Hospital, Xiamen University (Xiamen, China), and written informed consent was obtained from all subjects prior to the study start.

Patient consent for publication

Not applicable.

Competing interests

The authors declare that they have no competing interests.

References

1. Tsang CM, Lui VWY, Bruce JP, Pugh TJ and Lo KW: Translational genomics of nasopharyngeal cancer. Semin Cancer Biol, Sep 12, 2019 (Epub ahead of print).
2. Chen YP, Chan ATC, Le QT, Blanchard P, Sun Y and Ma J: Nasopharyngeal carcinoma. Lancet 394: 64-80, 2019.
3. Wilusz JE and Sharp PA: A circuitous route to noncoding RNA. Science 340: 440-441, 2013.
4. Wu J and Hann SS: Functions and roles of long-non-coding RNAs in human nasopharyngeal carcinoma. Cell Physiol Biochem 45: 1191-1204, 2018.
5. Anastasiadou E, Jacob LS and Slack FJ: Non-coding RNA networks in cancer. Nat Rev Cancer 18: 5-18, 2018.
6. Li LJ, Leng RX, Fan YG, Pan HF and Ye DQ: Translation of noncoding RNAs: Focus on lncRNAs, pri-miRNAs, and circRNAs. Exp Cell Res 361: 1-8, 2017.
7. Bhan A, Soleimani M and Mandal SS: Long noncoding RNA and cancer: A new paradigm. Cancer Res 77: 3965-3981, 2017.
8. Yang QQ and Deng YF: Long non-coding RNAs as novel biomarkers and therapeutic targets in head and neck cancers. Int J Clin Exp Pathol 7: 1286-1292, 2014.
9. Anfossi S, Fu X, Nagvekar R and Calin GA: MicroRNAs, regulatory messengers inside and outside cancer cells. Adv Exp Med Biol 1056: 87-108, 2018.
10. Zang J, Lu D and Xu A: The interaction of circRNAs and RNA binding proteins: An important part of circRNA maintenance and function. J Neurosci Res 98: 87-97, 2020.
11. Gong Z, Yang Q, Zeng Z, Zhang W, Li X, Zu X, Deng H, Chen P, Liao Q, Xiang B, *et al*: An integrative transcriptomic analysis reveals p53 regulated miRNA, mRNA, and lncRNA networks in nasopharyngeal carcinoma. Tumour Biol 37: 3683-3695, 2016.
12. Ma DD, Yuan LL and Lin LQ: lncRNA HOTAIR contributes to the tumorigenesis of nasopharyngeal carcinoma via up-regulating FASN. Eur Rev Med Pharmacol Sci 21: 5143-5152, 2017.
13. Zhang ZZ, Cao HC, Huang DL, Chen XF, Wan J and Zhang W: MicroRNA-200c plays an oncogenic role in nasopharyngeal carcinoma by targeting PTEN. Tumour Biol 39: 1010428317703655, 2017.
14. Shuai M, Hong J, Huang D, Zhang X and Tian Y: Upregulation of circRNA_0000285 serves as a prognostic biomarker for nasopharyngeal carcinoma and is involved in radiosensitivity. Oncol Lett 16: 6495-6501, 2018.
15. Livak KJ and Schmittgen TD: Analysis of relative gene expression data using real-time quantitative PCR and the 2(-Delta Delta C(T)) method. Methods 25: 402-408, 2001.
16. Paul P, Deka H, Malakar AK, Halder B and Chakraborty S: Nasopharyngeal carcinoma: Understanding its molecular biology at a fine scale. Eur J Cancer Prev 27: 33-41, 2018.
17. Nicolas FE: Role of ncRNAs in development, diagnosis and treatment of human cancer. Recent Pat Anticancer Drug Discov 12: 128-135, 2017.
18. Kristensen LS, Hansen TB, Venø MT and Kjems J: Circular RNAs in cancer: Opportunities and challenges in the field. Oncogene 37: 555-565, 2018.
19. Du WW, Zhang C, Yang W, Yong T, Awan FM and Yang BB: Identifying and characterizing circRNA-protein interaction. Theranostics 7: 4183-4191, 2017.
20. Liu M, Zhu K, Qian X and Li W: Identification of miRNA/mRNA-negative regulation pairs in nasopharyngeal carcinoma. Med Sci Monit 22: 2215-2234, 2016.
21. Zhang H, Liu J, Fu X and Yang A: Identification of key genes and pathways in tongue squamous cell carcinoma using bioinformatics analysis. Med Sci Monit 23: 5924-5932, 2017.
22. Lim SY, Yuzhalin AE, Gordon-Weeks AN and Muschel RJ: Targeting the CCL2-CCR2 signaling axis in cancer metastasis. Oncotarget 7: 28697-28710, 2016.
23. Fang ZQ, Zang WD, Chen R, Ye BW, Wang XW, Yi SH, Chen W, He F and Ye G: Gene expression profile and enrichment pathways in different stages of bladder cancer. Genet Mol Res 12: 1479-1489, 2013.
24. Okai I, Wang L, Gong L, Arko-Boham B, Hao L, Zhou X, Qi X, Hu J and Shao S: Overexpression of JAKMIP1 associates with Wnt/β-catenin pathway activation and promotes cancer cell proliferation in vitro. Biomed Pharmacother 67: 228-234, 2013.
25. Hu X, Zhao Y, Wei L, Zhu B, Song D, Wang J, Yu L and Wu J: CCDC178 promotes hepatocellular carcinoma metastasis through modulation of anoikis. Oncogene 36: 4047-4059, 2017.
26. Alajez NM, Lenarduzzi M, Ito E, Hui AB, Shi W, Bruce J, Yue S, Huang SH, Xu W, Waldron J, *et al*: MiR-218 suppresses nasopharyngeal cancer progression through downregulation of survivin and the SLIT2-ROBO1 pathway. Cancer Res 71: 2381-2391, 2011.
27. Ying J, Li H, Seng TJ, Langford C, Srivastava G, Tsao SW, Putti T, Murray P, Chan AT and Tao Q: Functional epigenetics identifies a protocadherin PCDH10 as a candidate tumor suppressor for nasopharyngeal, esophageal and multiple other carcinomas with frequent methylation. Oncogene 25: 1070-1080, 2006.
28. Cao JY, Liu L, Chen SP, Zhang X, Mi YJ, Liu ZG, Li MZ, Zhang H, Qian CN, Shao JY, *et al*: Prognostic significance and therapeutic implications of centromere protein F expression in human nasopharyngeal carcinoma. Mol Cancer 9: 237, 2010.